Behavioral/Cognitive

Human Sensory Cortex Contributes to the Long-Term Storage of Aversive Conditioning

Yuqi You, Joshua Brown, and Wen Li
Department of Psychology, Florida State University, Tallahassee, Florida 32306

Growing animal data evince a critical role of the sensory cortex in the long-term storage of aversive conditioning, following acquisition and consolidation in the amygdala. Whether and how this function is conserved in the human sensory cortex is nonetheless unclear. We interrogated this question in a human aversive conditioning study using multidimensional assessments of conditioning and long-term (15 d) retention. Conditioned stimuli (CSs; Gabor patches) were calibrated to differentially activate the parvocellular (P) and magnocellular (M) visual pathways, further elucidating cortical versus subcortical mechanisms. Full-blown conditioning and long-term retention emerged for M-biased CS (vs limited effects for P-biased CS), especially among anxious individuals, in all four dimensions assessed: threat appraisal (threat ratings), physiological arousal (skin conductance response), perceptual learning [discrimination sensitivity (d') and response speed], and cortical plasticity [visual evoked potentials (VEPs) and cortical current density]. Interestingly, while behavioral, physiological, and VEP effects were comparable at immediate and delayed assessments, the cortical substrates evolved markedly over time, transferring from high-order cortices [inferotemporal/fusiform cortex and orbitofrontal cortex (OFC)] immediately to the primary and secondary visual cortex after the delay. In sum, the contrast between P- and M-biased conditioning confirms privileged conditioning acquisition via the subcortical pathway while the immediate cortical plasticity lends credence to the triadic amygdala–OFC–fusiform network thought to underlie threat processing. Importantly, long-term retention of conditioning in the basic sensory cortices supports the conserved role of the human sensory cortex in the long-term storage of aversive conditioning.

Key words: **aversive conditioning; fear learning and memory; long-term memory; magnocellular and parvocellular visual pathways; neural plasticity; perceptual learning**

Significance Statement

A growing network of neural substrates has been identified in threat learning and memory. The sensory cortex plays a key role in long-term threat memory in animals, but such a function in humans remains unclear. To explore this problem, we conducted multidimensional assessments of immediate and delayed (15 d) effects of human aversive conditioning. Behavioral, physiological, and scalp electrophysiological data demonstrated conditioning effects and long-term retention. High-density EEG intracranial source analysis further revealed the cortical underpinnings, implicating high-order cortices immediately and primary and secondary visual cortices after the long delay. Therefore, while high-order cortices support aversive conditioning acquisition (i.e., threat learning), the human sensory cortex (akin to the animal homolog) underpins long-term storage of conditioning (i.e., long-term threat memory).

Introduction

The pressure to efficiently detect and respond to threat has motivated the evolution of adaptive neural machinery to support threat learning and memory. Aversive conditioning reliably generates associative threat learning and memory, underpinned by plastic changes in the amygdala (Pavlov, 1927; LeDoux, 2000). Recent work has further revealed plasticity in several cortical areas associated with various aspects of aversive conditioning, including the sensory cortex, insula, and prefrontal cortex (Antoniadis et al., 2007; Machado et al., 2009; Sehlmeyer et al., 2009; Fullana et al., 2016).

The sensory cortex has gained rapidly growing recognition as a critical neural substrate for associative threat learning and memory (Sehlmeyer et al., 2009; Miskovic and Keil, 2012; Li, 2014; Dunsmoor and Paz, 2015; McGann, 2015; Fullana et al., 2016; Grosso et al., 2017), reviving early pioneering findings of auditory cortical plasticity for conditioned stimuli (CSs; Galambos et al., 1956;

Received Sep. 3, 2020; revised Jan. 24, 2021; accepted Feb. 11, 2021.
Author contributions: Y.Y. and W.L. designed research; Y.Y. performed research; Y.Y. and W.L. analyzed data; Y.Y., J.B., and W.L. wrote the paper.
This research was supported by the National Institute of Mental Health Grant R01-MH-093413 (to W.L.).
The authors declare no competing financial interests.
Correspondence should be addressed to Wen Li at wenli@psy.fsu.edu or Yuqi You at you@psy.fsu.edu.
https://doi.org/10.1523/JNEUROSCI.2325-20.2021
Copyright © 2021 the authors

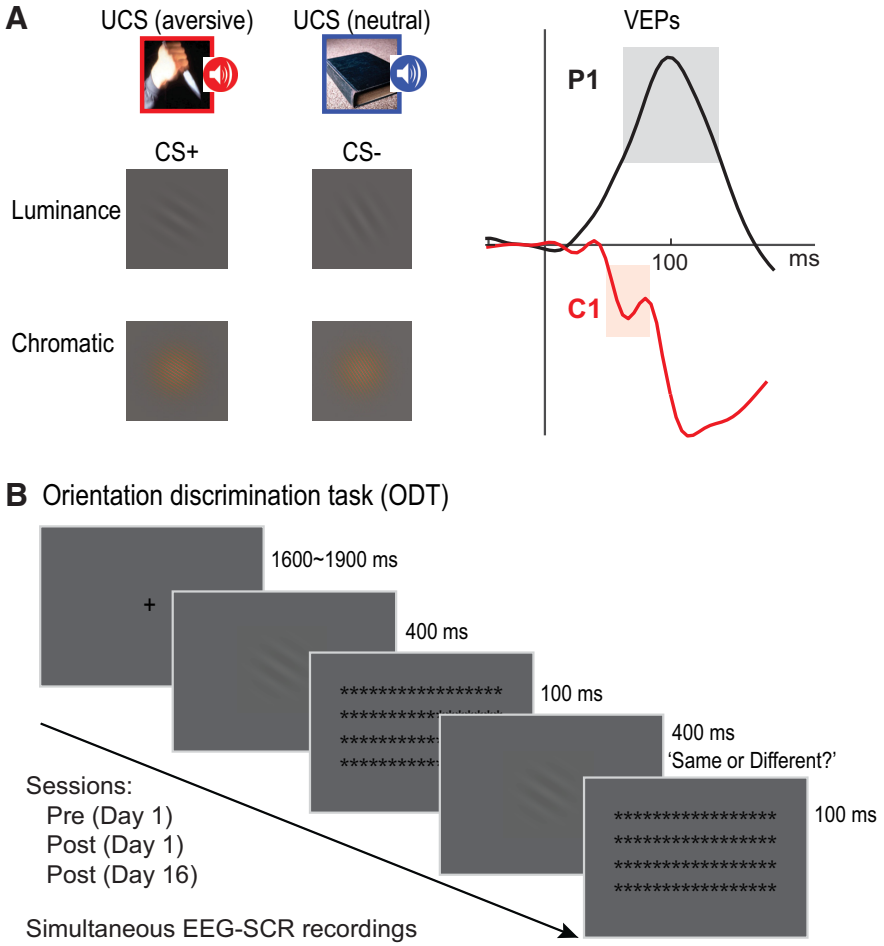

Figure 1. Experimental paradigm. ***A***, We calibrated three properties of the Gabor patches—chromaticity, luminance contrast, and spatial frequency—to generate a luminance stimulus type (achromatic, low spatial frequency, low luminance contrast) and a chromatic stimulus type (red-green isoluminant, high spatial frequency), thereby preferentially engaging M versus P visual pathways. Akin to their visual properties, these two types of stimuli are known to evoke distinct VEPs. To isolate a basic visual cortical response in the initial feedforward sweep, we focused on the first VEP they each elicit (i.e., P1 and C1 for the luminance and chromatic stimuli, respectively). ***B***, Paradigm of an ODT, which contained trials of two consecutively delivered Gabor patches of either the Same or Different orientation. The first Gabor patch was either the $CS^{+/-}$, and the second Gabor patch had either the same orientation (50%) or differed by 12° (50%) from the first Gabor patch. The task was performed at preconditioning, day 1 postconditioning, and day 16 postconditioning, while EEG and SCR were simultaneously recorded.

Kraus and Disterhoft, 1982; Diamond and Weinberger, 1984; Weinberger et al., 1984). Particularly, recent evidence has identified a potentially causal role of the sensory cortex in the formation and storage of long-term memory of aversive conditioning (Weinberger et al., 1993; Galván and Weinberger, 2002; Sacco and Sacchetti, 2010; Kwon et al., 2012; Grosso et al., 2015; Cambiaghi et al., 2016; Yang et al., 2016; Grosso et al., 2017). Such sensory cortical plasticity is found to accompany and potentially play a necessary role in perceptual learning of the CS, including improved stimulus detection and discrimination (Li et al., 2008; Padmala and Pessoa, 2008; Chapuis and Wilson, 2011; Wilson and Sullivan, 2011; Åhs et al., 2013; Aizenberg and Geffen, 2013; McGann, 2015). By facilitating stimulus analysis and accurate threat detection, such associative perceptual learning is likely to afford further ecological advantage to an organism.

Long-term memory storage of threat CSs in the sensory cortex can further support sensory cortex-based threat encoding (Weinberger, 2011; Miskovic and Keil, 2012; Li, 2014; Miskovic and Anderson, 2018; Li, 2019). That is, stored representation of acquired threat in the sensory cortex can be activated by feedforward transmission of CSs, triggering threat encoding in the sensory cortex (Krusemark and Li, 2011; Kumar et al., 2012; Krusemark et al., 2013; Krusemark and Li, 2013; Kragel et al., 2019). Akin to the "multiple-waves model" of emotion processing (Pessoa and Adolphs, 2010), this sensory cortical threat encoding represents an alternative, parallel mechanism to amygdala-centric threat processing (Phelps and LeDoux, 2005). However, to date, sensory cortical storage of long-term threat memory has been demonstrated in animals only. Furthermore, it remains equivocal whether extant evidence of threat processing in the human sensory cortex arises directly from the sensory cortex or consequent to amygdalar inputs.

To address these issues, we assessed threat learning and memory in a human aversive conditioning study including a retention test 15 d after conditioning. Four major domains of conditioning were assayed using a combination of threat appraisal, threat-related arousal [skin conductance response (SCR)], perceptual learning [using an orientation discrimination task (ODT)], and visual cortical plasticity [based on visual-evoked potentials (VEPs) and intracranial source estimation; Fig. 1]. We further calibrated visual properties of the CS (i.e., chromaticity, spatial frequency, and luminance contrast of Gabor patches) and created "luminance" and "chromatic" CSs (Fig. 1*A*). These two types of stimuli are known to bias the engagement of the parvocellular (P) versus magnocellular (M) visual pathways, preferentially mediating cortical versus subcortical signal transmission, respectively (Merigan and Maunsell, 1993; Lee, 2011, 2019). Accordingly, these stimuli would evoke distinct VEPs [e.g., a positive-going (P1) component and a negative-going (C1) component, respectively], allowing for differentiation of CS processing in parallel subcortical and cortical pathways (Fig. 1; Tobimatsu et al., 1995; Ellemberg et al., 2001; Schechter et al., 2005; Foxe et al., 2008). Our hypothesis testing centered on differences between $CS^{+/-}$ from preconditioning (Pre; baseline) to postconditioning (Post). We further examined their association with individual differences in anxiety, a critical modulatory factor of aversive conditioning (Zinbarg and Mohlman, 1998; Lissek et al., 2005).

Materials and Methods

Participants

Fifty-two right-handed college students (mean age, 19.5 years; 22 men) with normal or corrected-to-normal vision participated in the first of the two-session experiment. Forty-two of them returned for the second session ~15 d later (SD = 3.6 d). For EEG analysis, 5 of the 52 participants in the first session were excluded for excessive eye movements, severe

EEG artifact, and technical failures, resulting in a final N of 47 for the first session. Among the 42 participants who returned for the second session, 6 were excluded for the above reasons, resulting in a final number of 36 participants for the second session. All participants denied a history of severe head injury, psychological/neurologic disorders, or current use of psychotropic medication. All participants provided informed consent to participate in this study, which was approved by the University of Wisconsin Institutional Review Board.

Anxiety assessment

We assessed trait anxiety of the participants at the beginning of study using the Behavioral Inhibition Scale (BIS). The BIS is a 7-item self-report questionnaire (rated on a Likert scale of 1–4, with a total score of 7–28), measuring the strength of the behavioral inhibition system and threat sensitivity, known to reflect trait anxiety (Carver and White, 1994). This scale is neurobiologically motivated with high reliability and strong predictive validity of anxiety (Zinbarg and Mohlman, 1998; Gray and McNaughton, 2000).

Stimuli

Two types of Gabor patches (sinusoidal gratings multiplied by a Gaussian envelope; 9° × 9° in visual angles) were generated with specific visual properties that are known to preferentially stimulate the M and P pathways, respectively (Fig. 1*A*; Rudvin et al., 2000). To maximize the preferential activation of the M pathway, M-biased Gabor patches (i.e., luminance CSs) were achromatic, with low spatial frequency (<0.67 cycles/°) and low luminance contrast (6.9% Michelson contrast; luminance range, 20.16–23.14 cd/m^2). By contrast, P-biased Gabor patches (i.e., chromatic CSs) were chromatic (i.e., red-green) and isoluminant, and had high spatial frequency (>4 cycles/°). The red-green-gray isoluminant point was individually determined for each participant using heterochromatic flicker photometry (Bone and Landrum, 2004) with red, green, or gray squares alternatingly (at 30 Hz) presented on a CRT monitor.

Two grating orientations (for either luminance or chromatic Gabor patches) were differentially conditioned as CS$^+$ and CS$^-$ by pairing with aversive or neutral unconditioned stimuli (UCSs), respectively (Fig. 1*A*). The assignment of CS$^+$ orientation was counterbalanced across participants. Two sets of Gabor patches (33° and 57° or 123° and 147° clockwise from the vertical meridian) were included and counterbalanced across participants to exclude orientation-specific confounds. Aversive and neutral UCSs each consisted of seven pairs of simultaneously presented images and sounds. Images were selected from the International Affective Picture Set (Lang et al., 2008) and internet sources, depicting threatening scenes (e.g., knife put to throat; gun pointed to head) or household artifacts (e.g., whistle, cabinet). Fearful sounds (i.e., screams) were obtained from the fear subset of human affective vocalizations (Hawk et al., 2009), and neutral sounds consisted of pure tones at 300, 500, and 800 Hz.

All visual stimuli were presented on a gray background (21.65 cd/m^2) through a CRT monitor, which had been calibrated by first fitting a gamma function for each RGB channel based on sampled luminance values of each channel measured by a photometer, and then applying a reverse-gamma function on each RGB channel to achieve uniform steps of luminance increase using the Psychophysics Toolbox (Brainard, 1997). Stimulus presentation was linked to the refresh rate (60 Hz) of the CRT monitor and delivered using Cogent2000 software (Wellcome Laboratory of Neurobiology, UCL, London, UK) as implemented in MATLAB (MathWorks). Synchronization between stimulus display and data acquisition was verified using a photodiode placed at the center of the monitor screen.

Experiment procedure

The experiment included four phases with the first three, Pre (baseline), conditioning, and first postconditiong (Post day 1) taking place on day 1, and the fourth phase (second postconditioning) on day 16 (Post day 16). Note, we checked the success of conditioning on day 1 based on participants' report of CS–US contingency at the end of the session. Only those correctly reporting the contingency were invited back for the retention test on day 16.

Orientation discrimination task. To assess perceptual learning and memory via aversive conditioning, we implemented a challenging ODT at Pre, Post day 1, and Post day 16. Participants were seated ~60 cm from a CRT monitor with the head supported on a chin rest while simultaneous EEGs and SCRs were recorded. As illustrated in Fig. 1*B*, each trial began with a central fixation cross for a jittered duration of 1600–1900 ms. A CS (CS$^+$ or CS$^-$) Gabor patch then appeared for 400 ms, followed by a visual mask of 100 ms, which was replaced by a second Gabor patch for 400 ms and another visual mask of 100 ms. The orientation of the second Gabor patch was either the same as (i.e., "same" trial) or different from ("different" trial; 12° off clockwise or counterclockwise) the first Gabor patch with equal probability (50%). Participants were to report same or different for the pair. A total of 360 trials, 90 trials per condition (luminance/chromatic * CS$^+$/CS$^-$) were intermixed and randomly presented across three blocks. To minimize extinction potentially introduced by the repeated CS presentation, we inserted 10–12 reinforced CS trials randomly into the ODT at the two postconditioning phases (Post day 1 and Post day 16), as used in prior studies (Li et al., 2008; Padmala and Pessoa, 2008; Lissek et al., 2014; Onat and Büchel, 2015). These trials were excluded from the analysis.

We note that in contrast to typical conditioning manipulation, this reinforcement was designed to prevent extinction that otherwise would arise from the repeated CS presentation in the ODT. Accordingly, the reinforcement was sparse and delivered evenly across the task (approximately four trials/sub-block), in contrast to a typical conditioning paradigm with reinforcement rates >50% and reinforced trials concentrated at the beginning of the conditioning session. Such a sparse and evenly distributed reinforcement schedule was not expected to induce reliable conditioning effects. This notion was verified in an independent group of college students (N = 30) who underwent the same ODT (including the same reinforcement) but did not undergo the conditioning phase. Specifically, these participants showed no increase in risk, unpleasantness, or fear ratings for the CS$^+$ (vs CS$^-$), independently or in interaction with anxiety (p values >0.12). Also, they showed no improvement in orientation discrimination in either discrimination sensitivity (d') or response times (RTs) for the CS$^+$ (vs CS$^-$; p values >0.24).

Aversive conditioning. Luminance and chromatic CSs were presented in two separate blocks, each consisting of 20 trials (10 for CS$^+$, 10 for CS$^-$; 70% reinforcement). To ensure attention to the CS, participants were asked to indicate the CS orientation as either "steep" or "flat." The order of the luminance or chromatic block was counterbalanced across subjects. In each reinforced trial, a CS Gabor patch was centrally presented for 3000 ms, followed by simultaneous delivery of a threat or neutral UCS image (2000 ms) and sound (1500 ms). For the remaining 30% of trials, no UCS was presented following the CS.

Subjective ratings. At the end of the postconditioning phase on both days, participants were asked to rate on a visual analog scale (VAS) as to (1) how likely it was that a CS would be followed by a UCS (0−100% probability), (2) how pleasant a CS was (extremely unpleasant to extremely pleasant, 0–100), and (3) how fearful a CS was (not frightening at all to extremely frightening, 0–100). To minimize suggestibility and expectation biases, we avoided subjective ratings at the preconditioning phase.

EEG recording and analysis

The experiment took place in a dimly lit, electrically shielded room, where EEG data were recorded from a 96-channel (ActiveTwo, BioSemi) system at a 1024 Hz sampling rate. An electrooculogram was recorded at two eye electrodes at the outer canthus of each eye and one infraorbital to the left eye. EEG signals were referenced offline to the average of the 96 channels. EEG artifact detection and removal was achieved by the Fully Automated Statistical Thresholding for EEG artifact Rejection (FASTER) algorithm implemented in EEGLAB (Delorme and Makeig, 2004). Data were downsampled to 256 Hz, digital bandpass (0.1–40 Hz) filtered, and segmented into epochs of 200–300 ms around the onset of the CS (first Gabor patch). Epochs were rejected if their amplitude range, variance, and deviation exceeded the threshold of $z = \pm 3$ SDs, followed

by independent component analysis (ICA) using the Infomax algorithm (Bell and Sejnowski, 1995) to detect and remove artifactual components (e.g., muscular artifacts, eye blinks, and saccades, electrode "pop-offs"). Deviant channels within individually cleaned epochs were interpolated using the spherical spline interpolation function in EEGLAB. The final epochs were then corrected for the −200 ms baseline.

In keeping with the literature (Pourtois et al., 2005; Foxe et al., 2008; Thigpen et al., 2017), we observed maximal distributions of the C1 and P1 components at the midline occipital site Oz (collapsed across six surrounding electrodes; see Fig. 5*A*). We thus extracted P1 and C1 mean amplitudes at Oz, particularly, based on their rising slopes (P1, 78–129 ms; C1, 70–89 ms) as they maximize sensitivity to early visual feedforward processes (Ales et al., 2010; Kelly et al., 2013; Thigpen et al., 2017).

Exact low-resolution electromagnetic tomography source localization

Based on artifact-minimized VEP data from high-density EEG (hdEEG), we conducted intracranial source analyses using exact low-resolution electromagnetic tomography (eLORETA; Pascual-Marqui et al., 2011). The eLORETA algorithm on hdEEG data has been increasingly used for intracranial source estimation (Krusemark and Li, 2011, 2013; Whitton et al., 2018; Imperatori et al., 2019; Samogin et al., 2019; Clancy et al., 2020), having been cross-validated in multiple studies combining EEG-based LORETA with fMRI (Worrell et al., 2000; Vitacco et al., 2002; Mulert et al., 2004; Mobascher et al., 2009; Olbrich et al., 2009), positron emission tomography (Dierks et al., 2000; Pizzagalli et al., 2004), and intracranial recordings (Zumsteg et al., 2005).

The solution space consists of 6239 cortical gray matter voxels with a spatial resolution of 5 × 5 × 5 mm in a realistic head model (Fuchs et al., 2002) registered to standardized space from a digitized MRI at the Montreal Neurologic Institute (MNI). We estimated voxelwise current density during the C1 and P1 windows for each condition, which were then submitted to voxelwise statistical analyses. To minimize false-positive results in intracranial source localization, our laboratory has routinely applied two constraints in the analyses (Krusemark and Li, 2011, 2013; You and Li, 2016; Clancy et al., 2020). First, we constrained eLORETA analysis to the time windows and tests where surface ERP/EEG effects were significant (Thatcher et al., 2005). Second, we used Monte Carlo simulation based on the voxel spatial correlation in the data to set a corrected statistical threshold of $p < 0.05$. As such, applying the Gaussian filter widths estimated from our data (FWHMx = 0.75 mm, FWHMy = 0.82 mm, FWHMz = 0.75 mm), the voxel size (5 × 5 × 5 mm^3), and a connection radius (5 mm), we derived a corrected threshold consisting of a voxel-level $p < 0.01$ over four contiguous voxels for the P1 potential and $p < 0.05$ over eight contiguous voxels for the C1 potential (given its typically small amplitude). All coordinates are reported in the MNI space.

SCR recording and analysis

Skin conductance levels were continuously recorded (simultaneously with EEG recordings) during all phases of the experiment using the BioSemi ActiveTwo system. The continuous skin conductance recordings were downsampled to 256 Hz offline and analyzed using the SCR module of PsPM (version 3.1.1; Bach and Friston, 2013). The estimated SCR data were than high-pass filtered with a first-order Butterworth filter with a cutoff frequency of 0.05 Hz, downsampled further to 10 Hz, and normalized (z score transformed) for each participant. PsPM used a general linear model (based on a finite impulse response over 10 1 s time bins) to deconvolve rapid, overlapping, event-related SCRs. The resulting β values (regression coefficient) for each time bin were extracted for each condition, with the peak β value during the 1–9 s poststimulus window submitted to statistical analyses as the parameter estimate for evoked SCR.

Statistical analysis

Orientation discrimination performance in the ODT was characterized by the signal detection theory statistic d'. Extreme values (i.e., 0 or 1) of hit and false alarm rates were adjusted by [1 + 100 × hit (or false alarm) rate]/102 (Stanislaw and Todorov, 1999). RTs to all trials were extracted, with those <100 ms or 2 SDs above the subject's mean RT excluded from analysis. Given the negative polarity of the C1 component, we inverted the C1 magnitude (multiplied by −1) so that it could be compared with the P1 amplitude in statistical analyses.

As mentioned earlier, our hypotheses centered on conditioning, reflected by changes in differences between CS^+ and CS^- from preconditioning to postconditioning. We thus derived difference scores between CS^+ and CS^- (CS^+ – CS^-) for chromatic/luminance trials at Pre and Post sessions and submitted them into omnibus analyses of covariance (ANCOVAs; with Greenhouse–Geisser correction for nonsphericity) of Stimulus type (luminance/chromatic), Phase (Pre/Post), and Anxiety (BIS scores). Since evidence for conditioning rested on the effect of Phase, our hypothesis testing would follow marginal ($p < 0.1$) or significant Phase-related (simple or interaction) effects in the omnibus ANCOVAs. As such, effects not involving the Phase factor would not be further considered. Hypothesis testing in the follow-up tests would be thresholded at $p < 0.05$, following multiple comparisons using the false discovery rate (FDR) criterion (i.e., FDR $p < 0.05$). To note, for hypothesis testing corrected for multiple comparisons (e.g., FDR $p < 0.05$ used here), significant higher-order F tests do not provide additional protection for type I errors but rather overly restrict such errors (Wilcox, 1987). To strike a balance between type I and type II errors, our laboratory has routinely used significant or marginally significant F tests to justify and protect follow-up hypothesis testing (Clancy et al., 2020). As 10 subjects failed to return on day 16, we conducted analyses for day 1 and day 16 separately to preserve the sample size.

Results

Threat learning and memory

Threat appraisal

Threat ratings were conducted after conditioning only, and our key effects of interest concerned the main effects of CS (CS^+ vs CS^-). Separate three-way ANCOVAs of CS (CS^+/CS^-), Stimulus (luminance/chromatic), and Anxiety (BIS scores) on postconditioning ratings (risk, valence, and fear) revealed strong main effects of CS on both day 1 and day 16 (day 1: F values > 56.77, FDR p values < 0.001; day 16: F values > 37.18, FDR p values < 0.001, η_p^2 values ≥ 0.50). As illustrated in Fig. 2, on both days 1 and 16, CS^+ (vs CS^-) were rated as more unpleasant, more frightening, and more associated with the UCS. However, on neither day was there a main effect of Stimulus (day 1: F values < 2.70, p values > 0.10; day 16: F values < 3.47, p values > 0.07) or CS × Stimulus interaction (day 1: F values < 2.20, p values > 0.14; day 16: F values < 0.89, p values > 0.35) on these ratings. Anxiety did not modulate these effects of conditioning (p values > 0.09). In sum, these results supported immediate and lasting threat appraisal through aversive conditioning via both visual pathways.

Threat-related arousal

A three-way ANCOVA of Stimulus, Phase (Pre/Post day 1), and Anxiety on day 1 differential (CS^+ – CS^-) SCR yielded a marginally significant Stimulus × Phase interaction ($F_{(1,50)} = 3.29$, $p = 0.076$, $\eta_p^2 = 0.06$; Fig. 3). We then followed up with separate t tests for each stimulus type. The luminance CS^+ (vs CS^-) evoked greater SCR at postconditioning than preconditioning ($t_{(51)} = 2.52$; FDR $p < 0.05$; $d = 0.35$). However, no such SCR enhancement was observed for the chromatic CS^+ ($t_{(51)} = 0.42$, $p = 0.678$). A similar ANCOVA on day 16 (Phase: Pre/Post day 16) also revealed a trending Stimulus × Phase interaction ($F_{(1,39)} = 3.32$, $p = 0.076$, $\eta_p^2 = 0.08$). Similar follow-up t tests for the two stimulus types also demonstrated significantly elevated SCR to luminance CS^+ (vs CS^-) at day 16 postconditioning relative to preconditioning ($t_{(40)} = 2.92$; FDR $p < 0.01$; $d = 0.46$), while showing no change for chromatic CS^+ (vs CS^-; $t_{(40)} = -0.38$,

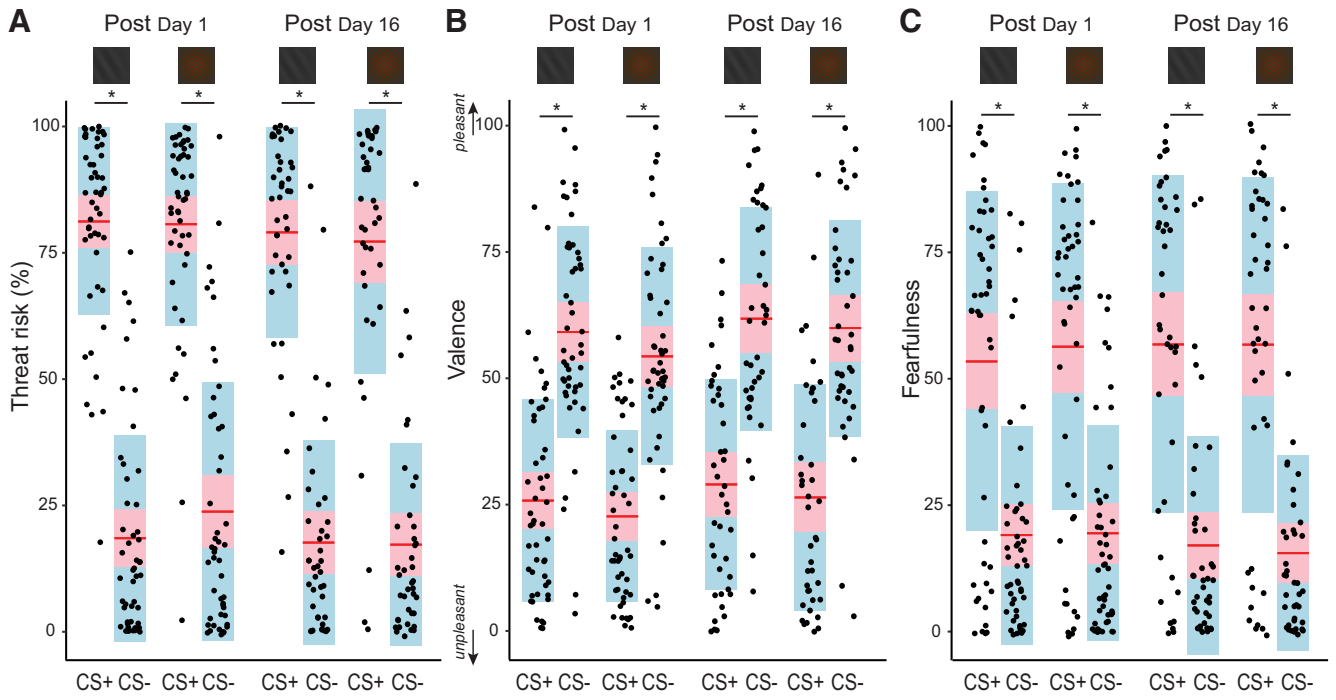

Figure 2. Subjective affective ratings after visual aversive conditioning. ***A–C***, On both day 1 and day 16, participants provided postconditioning ratings for the CS^+ and CS^- on the likelihood of an ensuing aversive UCS (***A***), affective valence (***B***), and fearfulness (***C***). Essentially identical for luminance and chromatic CS and for immediate and delayed assessments, CS^+ was rated as more associated with aversive UCS, more unpleasant, and more fearful than CS^-. The center red lines represent the mean values, with the red and blue areas representing the mean ± 1.96 × SEM and the mean ± 1 SD, respectively. $*p < 0.05$.

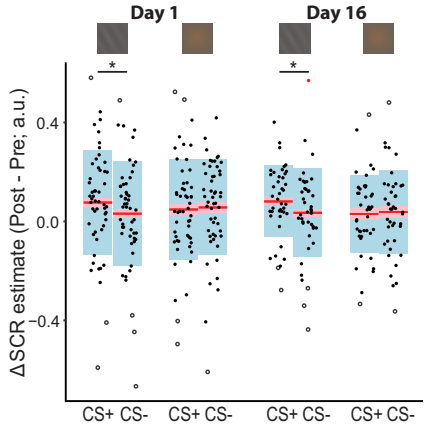

Figure 3. SCR effects of visual aversive conditioning. Participants showed greater SCR to luminance (but not chromatic) CS^+ (vs CS^-) at postconditioning on both day 1 and day 16. The center red lines represent the mean values, with the red and blue areas representing the 95% confidence interval and mean ± 1 SD, respectively. Open dots indicate regular outliers (greater than third quartile + 1.5 × interquartile range (IQR), or less than first quartile −1.5 × IQR); there was a single red dot indicating an extreme outlier (>3 IQR). These outliers appeared at both ends of the distributions. Exclusion of these outliers did not change the results such that they were included in the analyses for completeness. $*p < 0.05$.

$p = 0.708$). Therefore, only the M pathway-mediated CS exhibited threat arousal acquisition and memory. Last, anxiety had no effect on the SCR independently or interactively with the other factors (p values > 0.30).

Perceptual discrimination

Similar three-way (Stimulus × Phase × Anxiety) ANCOVAs were performed on differential (CS^+ – CS^-) ODT d' and RTs for day 1 and day 16. For day 1, there were no significant conditioning effects on RTs (F values < 2.62, p values > 0.11), but a significant three-way interaction (Stimulus × Phase × Anxiety; Phase: Pre/Post day 1) emerged for d' ($F_{(1,50)} = 8.27$, $p = 0.006$, $\eta_p^2 = 0.14$; Fig. 4*A*). Follow-up analyses indicated a significant Phase × Anxiety interaction for the luminance stimuli ($F_{(1,50)} = 5.22$, $p = 0.027$, $\eta_p^2 = 0.09$), substantiated by stronger d' increases for luminance CS^+ (vs CS^-) at postconditioning (vs preconditioning) among subjects with higher anxiety ($r = 0.31$; FDR $p < 0.05$). However, there were no conditioning effects for the chromatic stimuli (p values > 0.15). For day 16, similar ANCOVAs (Phase: Pre/Post day 16) showed no significant conditioning effects on d' (F values < 1.40, p values > 0.24), but a significant three-way interaction effect emerged for RTs ($F_{(1,40)} = 7.49$, $p = 0.009$, $\eta_p^2 = 0.16$; Fig. 4*B*). Follow-up analyses further isolated a Phase × Anxiety interaction for luminance CS ($F_{(1,40)} = 19.24$, $p < 0.001$, $\eta_p^2 = 0.33$), substantiated by faster RTs to luminance CS^+ (vs CS^-) at day 16 postconditioning (vs preconditioning) among anxious subjects ($r = -0.57$, FDR $p < 0.01$). However, again, there were no conditioning effects for chromatic CS (F values < 1.39, p values > 0.24). Together, in support of associative perceptual learning and memory, performance in the ODT was significantly improved for luminance CS at postconditioning among anxious subjects, manifested as higher d' on day 1 and faster RTs on day 16.

Neural plasticity associated with threat learning and memory

After confirming the signature VEPs for chromatic and luminance Gabor patches, we examined the effects of conditioning on differential (CS^+ – CS^-) VEPs in similar three-way (Phase × Stimulus × Anxiety) ANCOVAs for day 1 and day 16. We further estimated intracranial sources for significant VEP effects using eLORETA.

The ANCOVA for day 1 showed a trending three-way (Stimulus × Phase × Anxiety) interaction ($F_{(1,45)} = 3.23$, $p =$

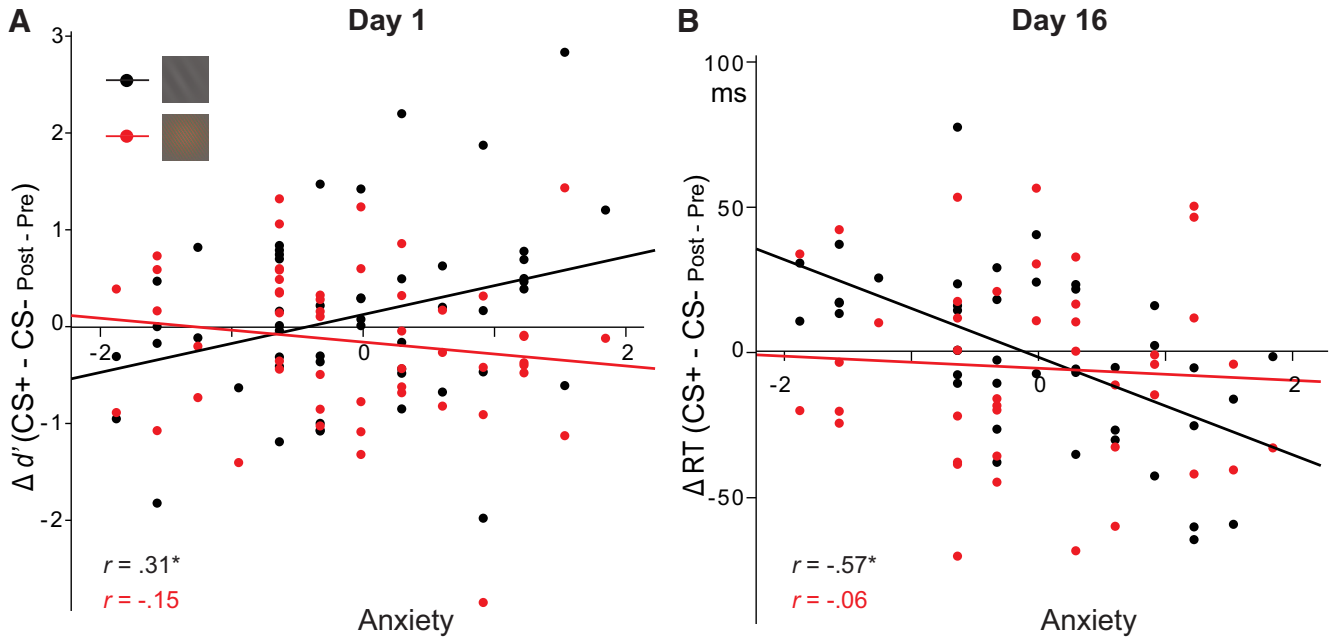

Figure 4. Perceptual effects of conditioning on orientation discrimination performance. ***A***, Immediate (day 1 postconditioning vs preconditioning) increase in d' to luminance CS^+ (vs CS^-; black dots), varying as a function of BIS scores (indexing trait anxiety). No effects were observed for the chromatic CS (red dots). ***B***, Faster RTs at day 16 postconditioning (vs preconditioning) to luminance but not chromatic CS^+ (vs CS^-), varying as a function of trait anxiety. $*p < 0.05$

0.079, $\eta_p^2 = 0.07$; Fig. 5*B*). Follow-up tests on P1 amplitudes revealed a significant Phase × Anxiety interaction evoked by luminance CS ($F_{(1,45)} = 5.74$, $p = 0.021$, $\eta_p^2 = 0.11$) and greater enhancement in P1 to luminance CS^+ (vs CS^-) at postconditioning (vs preconditioning) among anxious subjects ($r = 0.34$, $p = 0.021$). eLORETA and voxelwise regression analysis isolated the cortical source of this P1 effect in the visual cortex [right fusiform gyrus: peak, $x = 30$, $y = -40$, $z = -10$, $r = 0.45$, k = 77; right middle occipital gyrus: peak, $x = 45$, $y = -85$, $z = 5$, $r = 0.54$, k = 19; FDR p values < 0.05; right orbitofrontal cortex (OFC): peak, $x = 20$, $y = 35$, $z = -20$, $r = 0.52$, k = 64; FDR $p < 0.05$; Fig. 5*C*].

Follow-up tests on C1 magnitudes evoked by chromatic CS^+ (vs CS^-) showed a Phase effect ($F_{(1,45)} = 7.33$, $p = 0.010$, $\eta_p^2 = 0.14$): C1 magnitudes were enhanced for chromatic CS^+ (vs CS^-) at postconditioning (vs preconditioning). eLORETA then localized this effect to the striate and circumstriate visual cortices [primary visual cortex (V1)/secondary visual cortex (V2); peak: $x = 5$, $y = -70$, $z = 15$, $t_{(46)} = 2.69$, k = 10; FDR $p < 0.05$; Fig. 5*D*].

A similar ANCOVA for day 16 also showed a three-way interaction (Stimulus × Phase × Anxiety; $F_{(1,34)} = 4.05$, $p = 0.052$, $\eta_p^2 = 0.11$; Fig. 6*B*). Follow-up tests again revealed a Phase × Anxiety interaction on P1 amplitudes evoked by luminance stimuli ($F_{(1,34)} = 9.38$, $p = 0.004$, $\eta_p^2 = 0.22$): greater enhancement in P1 to luminance CS^+ (vs CS^-) at postconditioning (vs preconditioning) among anxious subjects ($r = 0.46$, $p = 0.004$). eLORETA isolated this P1 effect in the V1 and V2 (peak, $x = 0$, $y = -85$, $z = -5$, $r = 0.56$, k = 43; FDR p values < 0.05), the right middle occipital gyrus (peak, $x = 40$, $y = -90$, $z = 0$, $r = 61$, k = 22; FDR $p < 0.05$), and the left dorsolateral prefrontal cortex (DLPFC; peak, $x = -30$, $y = 40$, $z = 30$, $r = 0.57$, k = 42; FDR $p < 0.05$; Fig. 6*C*). However, no conditioning effects were observed for C1 evoked by chromatic stimuli (p values > 0.32).

Confirmatory analyses of threat memory (postconditioning day 1 vs day 16)

Finally, to further ascertain the long-term effects of conditioning, we directly compared the two Post sessions in similar ANCOVAs (Stimulus × Phase × Anxiety) on the dependent variables above, with the Phase factor containing the Post sessions on day 1 and day 16.

In keeping with the results above showing similar conditioning effects on threat appraisal, SCR, and scalp VEPs on both days, these ANCOVAs confirmed no significant phase-related effects: Phase (p values > 0.262), Stimulus × Phase (p values > 0.29), or Stimulus × Phase × Anxiety (p values > 0.36). There were marginal Phase × Anxiety interaction effects on valence ($p = 0.062$) and fear ratings ($p = 0.071$) but not on risk ratings ($p = 0.562$), reflecting somewhat greater modulation of anxiety on threat ratings on day 16 (vs day 1). These results were not discussed further for failing to reach the statistical significance for hypothesis testing. Overall, threat appraisal on both days indicate comparable immediate learning and long-term memory effects of conditioning.

Results above indicated that conditioning impacted different aspects of perceptual discrimination (of luminance CS^+) on day 1 and day 16. Indeed, the ANCOVA on RTs showed a significant three-way (Stimulus × Phase × Anxiety) interaction ($F_{(1,40)} = 5.18$, $p = 0.028$, $\eta_p^2 = 0.12$). Follow-up analyses revealed faster RTs to luminance CS^+ (vs CS^-) at day 16 (vs day 1) postconditioning among anxious participants ($r = -0.51$, $p = 0.001$). Interestingly, although conditioning effects on d' appeared on day 1 only, the ANCOVA on d' showed no significant Phase ($p = 0.470$) or Stimulus × Phase interaction ($p = 0.209$), or their interaction with anxiety (p values > 0.10), in addition to a marginal effect of Phase × Stimulus × Anxiety ($p = 0.098$). However, further follow-up tests on that marginal effect showed no effect of Phase × Anxiety interaction for either Stimulus type (p values > 0.18). In sum, these results thus suggest a significant increase in perceptual discrimination speed, but no significant change in accuracy, for luminance CS^+ at postconditioning from day 1 to day 16.

The results described above also indicated a shift in the intracranial sources of the P1 effect from day 1 to day 16. eLORETA

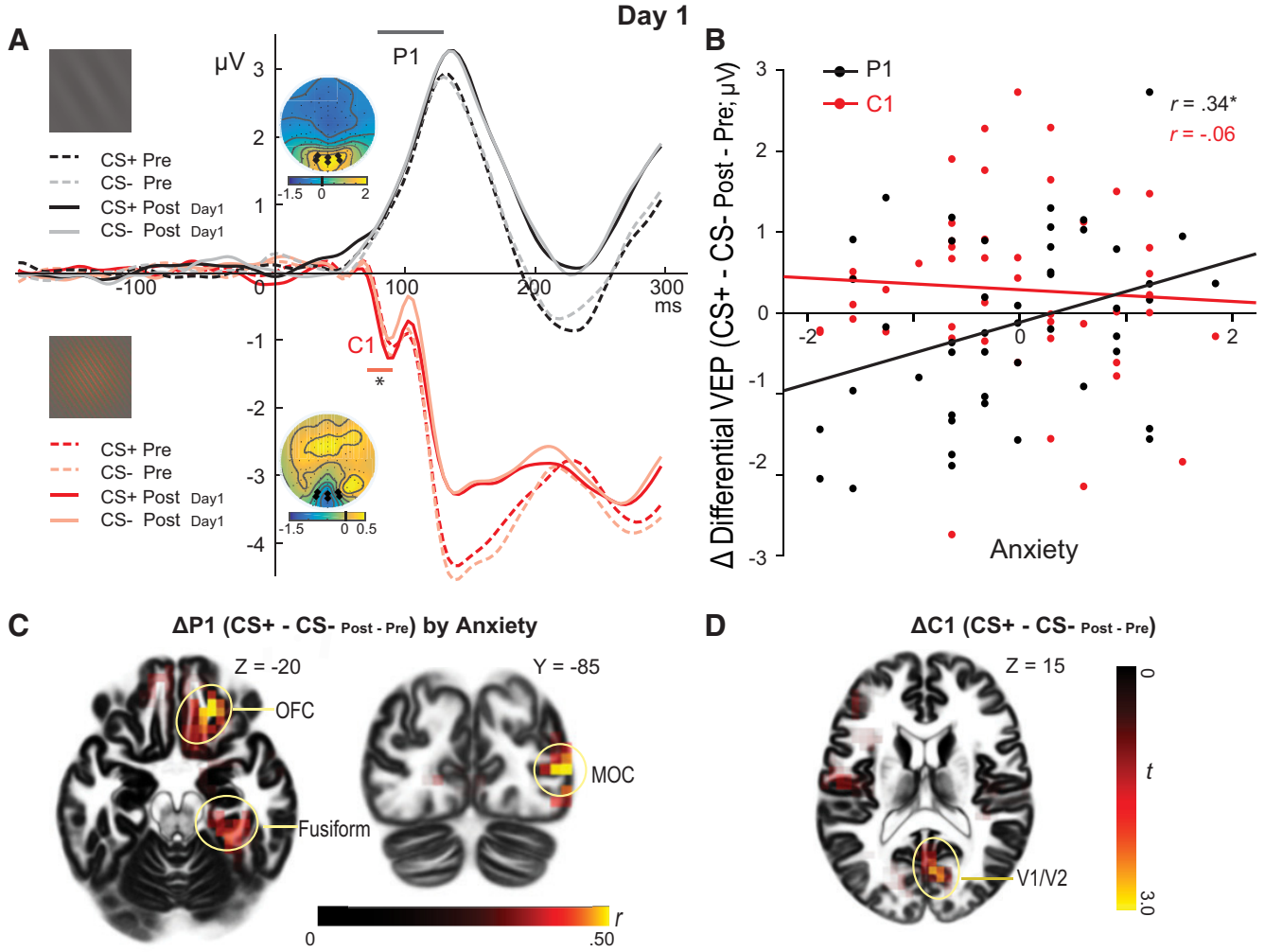

Figure 5. Immediate neural plasticity (day 1). ***A***, Grand average VEP waveforms at Oz show distinct P1 and C1 potentials at preconditioning (dashed lines) and postconditioning (solid lines) for luminance and chromatic CS, respectively. Temporal windows over the rising slopes of P1 and C1 are indicated by horizontal bars. C1 to chromatic CS^+ (vs CS^-) was significantly potentiated at day 1 postconditioning (vs preconditioning; $*p < 0.05$). Topographical maps are based on baseline recordings collapsed across CS^+ and CS^- trials, with the Oz electrodes highlighted as bold dots (top, P1; bottom, C1). ***B***, VEP (P1 and C1) changes postconditioning in relation to anxiety: enhancement in P1 amplitude (black dots) to CS^+ (vs CS^-) at postconditioning (vs preconditioning) positively correlated with anxiety, but not for C1 amplitudes (red dots). ***C***, eLORETA source estimation localized enhanced P1 in relation to anxiety in the OFC, temporal fusiform gyrus, and the middle occipital cortex (MOC). ***D***, eLORETA localized the enhanced C1 for CS^+ (vs CS^-) to the V1 and V2. $*p < 0.05$.

analysis, regressing changes in differential current density from day 1 to day 16 postconditioning [$CS^+ - CS^-$ (Post day 16 – Post day 1)] on anxiety (thresholded at $p < 0.05$; k = 8; FDR p values < 0.05), identified greater current density to CS^+ (vs CS^-) on day 16 (vs day 1) among anxious participants in the DLPFC (peak, $x = -25$, $y = 45$, $z = 25$, $r = 0.45$, k = 32; FDR p values < 0.05) and visual cortices (V1/V2; peak, $x = 0$, $y = -90$, $z = -15$, $r = 0.40$, k = 19; FDR p values < 0.05). These clusters appeared to be the same ones isolated in the comparison between preconditioning and day 16 postconditioning above, highlighting the neural substrates for long-term conditioning effects.

In summary, these results indicate that immediate conditioning effects in threat appraisal, SCR, and P1 persisted to day 16, maintaining the initial strengths. They also highlighted a specific increase in the speed of perceptual discrimination for luminance CS^+ and specific engagement of V1/V2 and DLPFC to support luminance CS^+ processing on day 16.

Additional analysis of the time course of conditioning on day 16

The different patterns of conditioning effects (especially in perceptual learning and the intracranial substrates) for day 1 and day 16 evinced unique processes involved in threat learning versus memory. We further clarified whether there were any conditioning effects induced by the reinforcement (designed to prevent extinction) in the ODT that could potentially contribute to the conditioning effects for the luminance CS on day 16. As the reinforced trials were evenly spread throughout the task (approximately four trials/sub-block across three sub-blocks), if they had induced conditioning on day 16, the effect should exhibit a time course of increasing strength indicating that conditioning had taken place. We analyzed this possible time course by dividing day 16 postconditioning data for the luminance condition by sub-block, which were then submitted to two-way ANCOVAs of Block (sub-blocks 1–3) and Anxiety on the difference scores. These analyses showed no significant effects of Block or Block × Anxiety interaction on differential SCR (p values > 0.29), RT (p values > 0.37) or VEP (p values > 0.41), and all effect sizes were minimal (F values < 1.22; η_p^2 values < 0.03). These time course results further corroborated the notion that the limited reinforcement in the ODT on day 16 (designed to prevent extinction) did not induce meaningful conditioning.

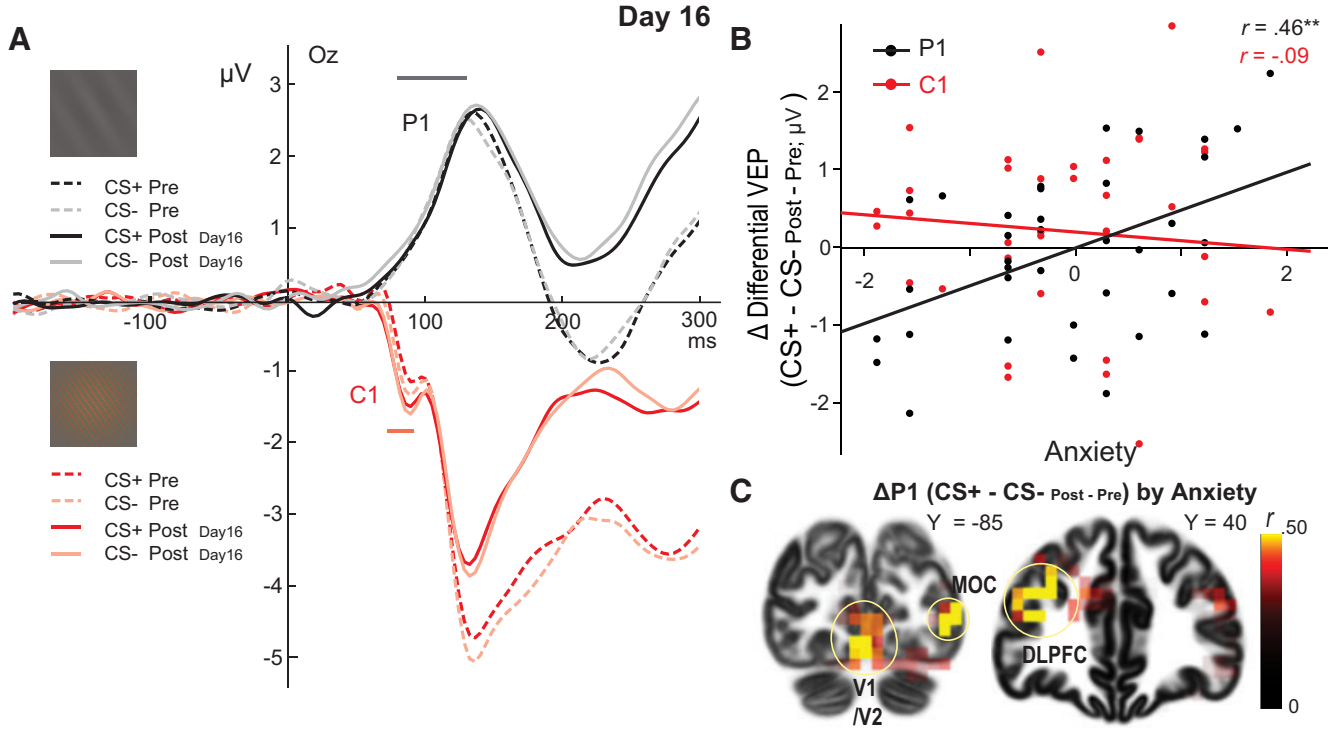

Figure 6. Long-term neural plasticity (day 16). ***A***, Grand average VEP waveforms at Oz for luminance and chromatic CS at preconditioning (dashed lines) and day 16 postconditioning (solid lines). Temporal windows over the rising slopes of P1 and C1 are indicated by horizontal bars. ***B***, Long-term effects of conditioning on P1 and C1 in relation to anxiety: enhancement in P1 amplitude (black dots) to CS^+ (vs CS^-) at postconditioning (vs preconditioning) positively correlated with anxiety, but not for C1 amplitudes (red dots). ***C***, eLORETA source estimation localized enhanced P1 in relation to anxiety to the V1/V2, middle occipital cortex (MOC), and the DLPFC. $**p < 0.01$.

Discussion

We conducted multidimensional assessments of immediate and long-term (15 d) effects of aversive conditioning using CS preferentially engaging M and P visual pathways. Conditioning via the M pathway resulted in immediate and long-term effects in all four domains assessed (i.e., threat appraisal, physiological arousal, perceptual learning, and cortical plasticity; Table 1). Importantly, cortical substrates (isolated based on hdEEG) exhibited remarkable temporal evolution, emerging in the OFC and fusiform cortex immediately after conditioning to give way to the V1 and V2 after the 15 d delay. Conditioning via the P pathway also heightened threat appraisal but induced only transient cortical plasticity and no perceptual learning or physiological arousal, confirming privileged aversive conditioning via the M pathway (and, by extension, the subcortical pathway). Together, these results elucidate human cortical contribution to aversive conditioning, implicating higher-order cortices in immediate learning and basic sensory cortices in long-term storage of conditioning.

P-biased input reaches the amygdala, the primary site for conditioning acquisition, via the ventral visual cortical stream, while M-biased input arrives at the amygdala preferentially via a subcortical (superior colliculus–pulvinar–amygdala) pathway (Merigan and Maunsell, 1993; Linke et al., 1999; Amaral et al., 2003; McFadyen et al., 2019). By pitting responses to chromatic (P-biased) and luminance (M-biased) CSs, we could differentiate cortical versus subcortical contributions to conditioning. Therefore, we carefully calibrated the visual properties of the CSs to differentially activate these pathways. The chromatic CSs were isoluminant red/green Gabor patches on an isoluminant gray background, with the isoluminance threshold determined for each participant using flicker photometry. Accordingly, orientation information that differentiated CS^+ and CS^- was contained solely in the color, which is known to efficiently activate the P but largely silence the M pathway (Merigan and Maunsell, 1993; Lee, 2011, 2019). Additionally, these Gabor patches contained only high-spatial frequency information (>4 cycles/°) to further minimize M pathway activation. By contrast, luminance CSs were achromatic/gray Gabor patches of low luminance contrast (6.9%) and low spatial frequency (0.67 cycles/°), set to the levels known to strongly stimulate the M pathway but largely silence the P pathway (i.e., <8% for luminance contrast; Tootell et al., 1988; Rudvin et al., 2000) and <1 cycle/° for spatial frequency (DeValois and DeValois, 1990). In validation of this stimulus manipulation, the luminance versus chromatic stimuli evoked distinct signature VEPs (i.e., a positive-going P1 vs a negative-going C1 component, respectively; Previc, 1988; Ellemberg et al., 2001; Schechter et al., 2005; Foxe et al., 2008).

Table 1. Multilevel effects of aversive conditioning (CS^+ vs CS^-)

CS type	Time	Threat appraisal	SCR	Perceptual learning	VEP
Luminance	Day 1	+	+	+* (*d′*)	+*
	Day 16	+	+	+* (RT)	+*
Chromatic	Day 1	+			+
	Day 16	+			

Perceptual learning was manifested in *d′* on day 1 and in RT on day 16.
+Significant increases from preconditioning to postconditioning.
*Changes from preconditioning to postconditioning correlated with BIS scores.

Conditioning for chromatic CSs (engaging the cortical pathway) resulted in the following limited effects: heightened threat appraisal (immediately and on day 16) and visual cortical response (immediately only) for the CS, but no change in physiological arousal or perceptual performance at either time point. Reflecting immediate visual cortical plasticity, chromatic CS^+ (vs CS^-) evoked greater C1 potential and current density in V1/V2 at ~80 ms, which is consistent with previous reports in humans

and monkeys (Stolarova et al., 2006; Thigpen et al., 2017; Li et al., 2019). The C1 potential is known to reflect the thalamus-to-V1 sensory transmission (Martínez et al., 1999; Di Russo et al., 2002). Therefore, the C1 (combined with V1/V2) effects here highlight heightened basic sensory processing of CS in the initial feedforward sweep. Echoing a previous report (Thigpen et al., 2017), these visual cortical effects did not last and disappeared by day 16. Absent heightened physiological arousal, this transient visual cortical plasticity may not reflect the updated visual cortical representation of CS (Sasikumar et al., 2018) but rather transient visual adaptation (e.g., heightened sensitivity) or saliency processing for the CS (Tolias et al., 2005; Keil et al., 2007). Notably, the lack of conditioning effects on day 16 further excluded the possibility that the limited reinforcement in the ODT could induce conditioning or reinstatement on day 16.

By contrast, conditioning for luminance CSs (preferentially engaging the subcortical pathway) yielded full-blown (in all four domains assessed) and lasting (until day 16) conditioning effects. These results confirmed the privileged M pathway (and, by extension, subcortical pathway) in mediating fear acquisition and the resulting long-term fear memory (Davis, 1992; LeDoux, 2000). The findings of immediate and lasting perceptual improvement for CS^+ can contribute to the burgeoning and yet controversial literature on human conditioning-induced (i.e., associative) perceptual learning and memory (Li et al., 2008; Åhs et al., 2013; Parma et al., 2015; Rhodes et al., 2018; Friedl and Keil, 2020). First, this associative perceptual learning and memory positively correlated with trait anxiety (known to enhance aversive conditioning; Lissek et al., 2005), highlighting its relevance to fear and origin in aversive conditioning. In addition, the covariation between such learning and anxiety suggests that uneven representation of anxious participants in prior studies (generally of small samples) could contribute to their inconsistent findings. Importantly, this close covariation lends direct support to recent theories promoting the role of perceptual processes in aversive conditioning and anxiety (Li et al., 2008; Dunsmoor and Paz, 2015; Li, 2019).

Second, immediate and delayed perceptual effects were manifested in different perceptual aspects (i.e., d') and response speed, respectively. These discrepancies (and relatedly, the controversial human literature) can find a viable explanation in the striking differences in immediate versus delayed neural substrates. Specifically, immediate plasticity in higher-order (OFC and fusiform) cortices could refine visual analysis and thus improve discrimination accuracy, whereas delayed plasticity in V1/V2 could facilitate basic sensory processing and thus increase response speed.

While the neural substrates evolved drastically over time, they were similarly modulated by trait anxiety and coupled with enhanced scalp P1 amplitude. The latter could reflect perceptual categorization of CS^+ versus CS^- in early sensory processing (Forscher et al., 2016; Meynadasy et al., 2020). Importantly, the distinct loci for immediate versus delayed plasticity highlight different neural and cognitive processes involved in threat learning and long-term memory. Specifically, except for a small cluster in the middle occipital gyrus, known for early object processing (Ishai et al., 2000), which was present throughout, the immediate substrates included the higher-order inferotemporal (fusiform) visual cortex and the OFC, while the delayed substrates involved the bilateral V1/V2 and left DLPFC. The immediate substrates conform to the frontal-posterior-cortical circuitry increasingly implicated in aversive conditioning, which is thought to mediate dynamic interaction between sensory encoding and cognitive evaluation of CS (Steinberg et al., 2012; Petro et al., 2017; Abend et al., 2020). Specifically, the inferotemporal cortex and OFC are densely connected via bidirectional axons, which could mediate the efficient processing of M-biased stimuli (Bar et al., 2006; Kveraga et al., 2007). Furthermore, these two structures are densely connected with the amygdala (excluded from source analysis given its deep location and subcortical nature), forming a triadic amygdala–OFC–temporal-cortex circuit to support the integration of sensory features and emotional significance (Ghashghaei and Barbas, 2002). Interestingly, we demonstrated that this OFC–fusiform circuit was right lateralized, underscoring the right hemisphere dominance in threat processing (Adolphs et al., 1996; Borod et al., 1998; Forscher and Li, 2012).

Overtime, this long-range frontal-posterior-cortical circuit appeared to undergo substantial rewiring by involving V1/V2 and DLPFC to support long-term retention. Akin to the rich animal evidence of a critical (and potentially causal) role of the primary/secondary cortex in the long-term storage of aversive conditioning (Weinberger, 2004; Li, 2014; McGann, 2015; Grosso et al., 2017), the prominence of the basic sensory cortex in this delayed circuit provides one of the first pieces of human evidence for that idea. The increased current density in the primary and secondary sensory cortices to CS could underpin "acquired associative representations" (AARs) of the CS (Weinberger, 2004; Li, 2014), which, in animals, can take the form of augmented response, enlarged receptive field, and/or sharpened tuning for the CS sensory features (e.g., grating orientation, tone frequency; Weinberger, 2007, 2011). Enduring AARs arising from lasting sensory cortical plasticity via aversive conditioning can be a neural mechanism for sensory cortical encoding of acquired threat: the CS cue, even long after the initial encounter, can activate its AAR to enable threat encoding in the initial feedforward sensory sweep (Sasikumar et al., 2018; Li et al., 2019).

Finally, the inclusion of the left DLPFC in the delayed circuit concurs with the increasingly recognized role of the DLPFC in various long-term memory processes (Blumenfeld and Ranganath, 2006; Hamidi et al., 2009; Manenti et al., 2010), with the left DLPFC particularly involved in emotional memory (Dolcos et al., 2004; Ferrari and Balconi, 2011). In light of its additional role in cognitive appraisal of emotion (Ochsner and Gross, 2008; Golkar et al., 2012) as well as attention and emotion regulation (Buschman and Miller, 2007), we surmise that the left DLPFC would support memory retrieval and regulatory processing of the CS.

The copious literature notwithstanding, contribution of the sensory cortex to threat learning and memory remains elusive in humans. Here, our findings provide important insights into this underexplored problem, underscoring high-order cortices in threat learning and, importantly, the conserved role of human primary/secondary sensory cortical cortices in long-term threat memory. Beyond that, the evolutionary expansion of human PFC has promoted PFC participation in conditioning, culminating in a sensory–prefrontal-cortical circuit to support complex and flexible processing of threat in humans.

References

Abend R, Gold AL, Britton JC, Michalska KJ, Shechner T, Sachs JF, Winkler AM, Leibenluft E, Averbeck BB, Pine DS (2020) Anticipatory threat responding: associations with anxiety, development, and brain structure. Biol Psychiatry 87:916–925.

Adolphs R, Damasio H, Tranel D, Damasio AR (1996) Cortical systems for the recognition of emotion in facial expressions. J Neurosci 16:7678–7687.

Åhs F, Miller SS, Gordon AR, Lundström JN (2013) Aversive learning increases sensory detection sensitivity. Biol Psychol 92:135–141.

Aizenberg M, Geffen MN (2013) Bidirectional effects of aversive learning on perceptual acuity are mediated by the sensory cortex. Nat Neurosci 16:994–996.

Ales JM, Yates JL, Norcia AM (2010) V1 is not uniquely identified by polarity reversals of responses to upper and lower visual field stimuli. Neuroimage 52:1401–1409.

Amaral DG, Behniea H, Kelly JL (2003) Topographic organization of projections from the amygdala to the visual cortex in the macaque monkey. Neuroscience 118:1099–1120.

Antoniadis EA, Winslow JT, Davis M, Amaral DG (2007) Role of the primate amygdala in fear-potentiated startle: effects of chronic lesions in the rhesus monkey. J Neurosci 27:7386–7396.

Bach DR, Friston KJ (2013) Model-based analysis of skin conductance responses: towards causal models in psychophysiology. Psychophysiology 50:15–22.

Bar M, Kassam KS, Ghuman AS, Boshyan J, Schmid AM, Schmidt AM, Dale AM, Hämäläinen MS, Marinkovic K, Schacter DL, Rosen BR, Halgren E (2006) Top-down facilitation of visual recognition. Proc Natl Acad Sci U S A 103:449–454.

Bell AJ, Sejnowski TJ (1995) An information-maximization approach to blind separation and blind deconvolution. Neural Comput 7:1129–1159.

Blumenfeld RS, Ranganath C (2006) Dorsolateral prefrontal cortex promotes long-term memory formation through its role in working memory organization. J Neurosci 26:916–925.

Bone RA, Landrum JT (2004) Heterochromatic flicker photometry. Arch Biochem Biophys 430:137–142.

Borod JC, Cicero BA, Obler LK, Welkowitz J, Erhan HM, Santschi C, Grunwald IS, Agosti RM, Whalen JR (1998) Right hemisphere emotional perception: evidence across multiple channels. Neuropsychology 12:446–458.

Brainard DH (1997) The psychophysics toolbox. Spat Vis 10:433–436.

Buschman TJ, Miller EK (2007) Top-down versus bottom-up control of attention in the prefrontal and posterior parietal cortices. science 315:1860–1862.

Cambiaghi M, Grosso A, Likhtik E, Mazziotti R, Concina G, Renna A, Sacco T, Gordon JA, Sacchetti B (2016) Higher-order sensory cortex drives basolateral amygdala activity during the recall of remote, but not recently learned fearful memories. J Neurosci 36:1647–1659.

Carver CS, White TL (1994) Behavioral inhibition, behavioral activation, and affective responses to impending reward and punishment: the BIS/BAS scales. J Pers Soc Psychol. 67:319–333.

Chapuis J, Wilson DA (2011) Bidirectional plasticity of cortical pattern recognition and behavioral sensory acuity. Nat Neurosci 15:155–161.

Clancy KJ, Albizu A, Schmidt NB, Li W (2020) Intrinsic sensory disinhibition contributes to intrusive re-experiencing in combat veterans. Sci Rep 10:936.

Davis M (1992) The role of the amygdala in fear and anxiety. Annu Rev Neurosci 15:353–375.

Delorme A, Makeig S (2004) EEGLAB: an open source toolbox for analysis of single-trial EEG dynamics including independent component analysis. J Neurosci Methods 134:9–21.

DeValois RL, DeValois KK (1990) Spatial vision. New York: Oxford UP.

Di Russo F, Martínez A, Sereno MI, Pitzalis S, Hillyard SA (2002) Cortical sources of the early components of the visual evoked potential. Hum Brain Mapp 15:95–111.

Diamond DM, Weinberger NM (1984) Physiological plasticity of single neurons in auditory cortex of the cat during acquisition of the pupillary conditioned response: II. Secondary field (AII). Behav Neurosci 98:189–210.

Dierks T, Jelic V, Pascual-Marqui RD, Wahlund L-O, Julin P, Linden DE, Maurer K, Winblad B, Nordberg A (2000) Spatial pattern of cerebral glucose metabolism (PET) correlates with localization of intracerebral EEG-generators in Alzheimer's disease. Clin Neurophysiol 111:1817–1824.

Dolcos F, LaBar KS, Cabeza R (2004) Dissociable effects of arousal and valence on prefrontal activity indexing emotional evaluation and subsequent memory: an event-related fMRI study. Neuroimage 23:64–74.

Dunsmoor JE, Paz R (2015) Fear generalization and anxiety: behavioral and neural mechanisms. Biol Psychiatry 78:336–343.

Ellemberg D, Hammarrenger B, Lepore F, Roy MS, Guillemot JP (2001) Contrast dependency of VEPs as a function of spatial frequency: the parvocellular and magnocellular contributions to human VEPs. Spat Vis 15:99–111.

Ferrari C, Balconi M (2011) DLPFC implication in memory processing of affective information. A look on anxiety trait contribution. Neuropsychol Trends April:53–70.

Forscher EC, Li W (2012) Hemispheric asymmetry and visuo-olfactory integration in perceiving subthreshold (micro) fearful expressions. J Neurosci 32:2159–2165.

Forscher EC, Zheng Y, Ke Z, Folstein J, Li W (2016) Decomposing fear perception: a combination of psychophysics and neurometric modeling of fear perception. Neuropsychologia 91:254–261.

Foxe JJ, Strugstad EC, Sehatpour P, Molholm S, Pasieka W, Schroeder CE, McCourt ME (2008) Parvocellular and magnocellular contributions to the initial generators of the visual evoked potential: high-density electrical mapping of the "C1" component. Brain Topogr 21:11–21.

Friedl WM, Keil A (2020) Effects of experience on spatial frequency tuning in the visual system: behavioral, visuocortical, and alpha-band responses. J Cogn Neurosci 32:1153–1169.

Fuchs M, Kastner J, Wagner M, Hawes S, Ebersole JS (2002) A standardized boundary element method volume conductor model. Clin Neurophysiol 113:702–712.

Fullana M, Harrison B, Soriano-Mas C, Vervliet B, Cardoner N, Àvila-Parcet A, Radua J (2016) Neural signatures of human fear conditioning: an updated and extended meta-analysis of fMRI studies. Mol Psychiatry 21:500–508.

Galambos R, Sheatz G, Vernier VG (1956) Electrophysiological correlates of a conditioned response in cats. Science 123:376–377.

Galván VV, Weinberger NM (2002) Long-term consolidation and retention of learning-induced tuning plasticity in the auditory cortex of the guinea pig. Neurobiol Learn Mem 77:78–108.

Ghashghaei H, Barbas H (2002) Pathways for emotion: interactions of prefrontal and anterior temporal pathways in the amygdala of the rhesus monkey. Neuroscience 115:1261–1279.

Golkar A, Lonsdorf TB, Olsson A, Lindstrom KM, Berrebi J, Fransson P, Schalling M, Ingvar M, Öhman A (2012) Distinct contributions of the dorsolateral prefrontal and orbitofrontal cortex during emotion regulation. PLoS One 7:e48107.

Gray JA, McNaughton N (2000) The Neuropsychology of anxiety:An enquiry into the functions of the septo-hippocampal system, Ed 2. Oxford, UK: Oxford UP.

Grosso A, Cambiaghi M, Renna A, Milano L, Merlo GR, Sacco T, Sacchetti B (2015) The higher order auditory cortex is involved in the assignment of affective value to sensory stimuli. Nat Commun 6:8886.

Grosso A, Cambiaghi M, Milano L, Renna A, Sacco T, Sacchetti B (2017) Region-and layer-specific activation of the higher order auditory cortex Te2 after remote retrieval of fear or appetitive memories. Cereb Cortex 27:3140–3151.

Hamidi M, Tononi G, Postle BR (2009) Evaluating the role of prefrontal and parietal cortices in memory-guided response with repetitive transcranial magnetic stimulation. Neuropsychologia 47:295–302.

Hawk ST, Van Kleef GA, Fischer AH, Van Der Schalk J (2009) Worth a thousand words": absolute and relative decoding of nonlinguistic affect vocalizations. Emotion 9:293–305.

Imperatori C, Farina B, Adenzato M, Valenti EM, Murgia C, Della Marca G, Brunetti R, Fontana E, Ardito RB (2019) Default mode network alterations in individuals with high-trait-anxiety: an EEG functional connectivity study. J Affect Disord 246:611–618.

Ishai A, Ungerleider LG, Martin A, Haxby JV (2000) The representation of objects in the human occipital and temporal cortex. J Cogn Neurosci 12:35–51.

Keil A, Stolarova M, Moratti S, Ray WJ (2007) Adaptation in human visual cortex as a mechanism for rapid discrimination of aversive stimuli. Neuroimage 36:472–479.

Kelly SP, Schroeder CE, Lalor EC (2013) What does polarity inversion of extrastriate activity tell us about striate contributions to the early VEP? A comment on Ales et al. (2010). Neuroimage 76:442–445.

Kragel PA, Reddan MC, LaBar KS, Wager TD (2019) Emotion schemas are embedded in the human visual system. Sci Adv 5:eaaw4358.

Kraus N, Disterhoft JF (1982) Response plasticity of single neurons in rabbit auditory association cortex during tone-signalled learning. Brain Res 246:205–215.

Krusemark EA, Li W (2011) Do all threats work the same way? Divergent effects of fear and disgust on sensory perception and attention. J Neurosci 31:3429–3434.

Krusemark EA, Li W (2013) From early sensory specialization to later perceptual generalization: dynamic temporal progression in perceiving individual threats. J Neurosci 33:587–594.

Krusemark EA, Novak LR, Gitelman DR, Li W (2013) When the sense of smell meets emotion: anxiety-state-dependent olfactory processing and neural circuitry adaptation. J Neurosci 33:15324–15332.

Kumar S, von Kriegstein K, Friston K, Griffiths TD (2012) Features versus feelings: dissociable representations of the acoustic features and valence of aversive sounds. J Neurosci 32:14184–14192.

Kveraga K, Boshyan J, Bar M (2007) Magnocellular projections as the trigger of top-down facilitation in recognition. J Neurosci 27:13232–13240.

Kwon J-T, Jhang J, Kim H-S, Lee S, Han J-H (2012) Brain region-specific activity patterns after recent or remote memory retrieval of auditory conditioned fear. Learn Mem 19:487–494.

Lang P, Bradley M, Cuthbert B (2008) International affective picture system (IAPS): affective ratings of pictures and instruction manual: technical report, A-6. Gainesville, FL: National Institute of Mental Health, Center for the Study of Emotion & Attention.

LeDoux JE (2000) Emotion circuits in the brain. Annu Rev Neurosci 23:155–184.

Lee BB (2011) Visual pathways and psychophysical channels in the primate. J Physiol 589:41–47.

Lee BB (2019) Sensitivity to chromatic and luminance contrast and its neuronal substrates. Curr Opin Behav Sci 30:156–162.

Li W (2014) Learning to smell danger: acquired associative representation of threat in the olfactory cortex. Front Behav Neurosci 8:98.

Li W (2019) Perceptual mechanisms of anxiety and its disorders. In: Cambridge handbook of anxiety and related disorders (Olatunji B, ed), Cambridge, UK: Cambridge UP.

Li W, Howard JD, Parrish TB, Gottfried JA (2008) Aversive learning enhances perceptual and cortical discrimination of indiscriminable odor cues. Science 319:1842–1845.

Li Z, Yan A, Guo K, Li W (2019) Fear-related signals in the primary visual cortex. Curr Biol 29:4078–4083.e2.

Linke R, De Lima A, Schwegler H, Pape HC (1999) Direct synaptic connections of axons from superior colliculus with identified thalamo-amygdaloid projection neurons in the rat: possible substrates of a subcortical visual pathway to the amygdala. J Comp Neurol 403:158–170.

Lissek S, Powers AS, McClure EB, Phelps EA, Woldehawariat G, Grillon C, Pine DS (2005) Classical fear conditioning in the anxiety disorders: a meta-analysis. Behav Res Ther 43:1391–1424.

Lissek S, Bradford DE, Alvarez RP, Burton P, Espensen-Sturges T, Reynolds RC, Grillon C (2014) Neural substrates of classically conditioned fear-generalization in humans: a parametric fMRI study. Soc Cogn Affect Neurosci 9:1134–1142.

Machado CJ, Kazama AM, Bachevalier J (2009) Impact of amygdala, orbital frontal, or hippocampal lesions on threat avoidance and emotional reactivity in nonhuman primates. Emotion 9:147–163.

Manenti R, Cotelli M, Calabria M, Maioli C, Miniussi C (2010) The role of the dorsolateral prefrontal cortex in retrieval from long-term memory depends on strategies: a repetitive transcranial magnetic stimulation study. Neuroscience 166:501–507.

Martínez A, Anllo-Vento L, Sereno MI, Frank LR, Buxton RB, Dubowitz D, Wong EC, Hinrichs H, Heinze HJ, Hillyard SA (1999) Involvement of striate and extrastriate visual cortical areas in spatial attention. Nat Neurosci 2:364–369.

McFadyen J, Mattingley JB, Garrido MI (2019) An afferent white matter pathway from the pulvinar to the amygdala facilitates fear recognition. Elife 8:e40766.

McGann JP (2015) Associative learning and sensory neuroplasticity: how does it happen and what is it good for? Learn Mem 22:567–576.

Merigan WH, Maunsell JH (1993) How parallel are the primate visual pathways? Annu Rev Neurosci 16:369–402.

Meynadasy M, Clancy K, Ke Z, Simon J, Wu W, Li W (2020) Impaired early visual categorization of fear in social anxiety. Psychophysiology 57: e13509.

Miskovic V, Anderson A (2018) Modality general and modality specific coding of hedonic valence. Curr Opin Behav Sci 19:91–97.

Miskovic V, Keil A (2012) Acquired fears reflected in cortical sensory processing: a review of electrophysiological studies of human classical conditioning. Psychophysiology 49:1230–1241.

Mobascher A, Brinkmeyer J, Warbrick T, Musso F, Wittsack H-J, Stoermer R, Saleh A, Schnitzler A, Winterer G (2009) Fluctuations in electrodermal activity reveal variations in single trial brain responses to painful laser stimuli—a fMRI/EEG study. Neuroimage 44:1081–1092.

Mulert C, Jäger L, Schmitt R, Bussfeld P, Pogarell O, Möller H-J, Juckel G, Hegerl U (2004) Integration of fMRI and simultaneous EEG: towards a comprehensive understanding of localization and time-course of brain activity in target detection. Neuroimage 22:83–94.

Ochsner KN, Gross JJ (2008) Cognitive emotion regulation: insights from social cognitive and affective neuroscience. Curr Dir Psychol Sci 17:153–158.

Olbrich S, Mulert C, Karch S, Trenner M, Leicht G, Pogarell O, Hegerl U (2009) EEG-vigilance and BOLD effect during simultaneous EEG/fMRI measurement. Neuroimage 45:319–332.

Onat S, Büchel C (2015) The neuronal basis of fear generalization in humans. Nat Neurosci 18:1811–1818.

Padmala S, Pessoa L (2008) Affective learning enhances visual detection and responses in primary visual cortex. J Neurosci 28:6202–6210.

Parma V, Ferraro S, Miller SS, Åhs F, Lundström JN (2015) Enhancement of odor sensitivity following repeated odor and visual fear conditioning. Chem Senses 40:497–506.

Pascual-Marqui RD, Lehmann D, Koukkou M, Kochi K, Anderer P, Saletu B, Tanaka H, Hirata K, John ER, Prichep L, Biscay-Lirio R, Kinoshita T (2011) Assessing interactions in the brain with exact low-resolution electromagnetic tomography. Philos Trans A Math Phys Eng Sci 369:3768–3784.

Pavlov IP (1927) Conditioned reflexes (Anrep GV, translator). London: Oxford.

Pessoa L, Adolphs R (2010) Emotion processing and the amygdala: from a "low road" to "many roads" of evaluating biological significance. Nat Rev Neurosci 11:773–782.

Petro NM, Gruss LF, Yin S, Huang H, Miskovic V, Ding M, Keil A (2017) Multimodal imaging evidence for a frontoparietal modulation of visual cortex during the selective processing of conditioned threat. J Cogn Neurosci 29:953–967.

Phelps EA, LeDoux JE (2005) Contributions of the amygdala to emotion processing: from animal models to human behavior. Neuron 48:175–187.

Pizzagalli D, Oakes T, Fox A, Chung M, Larson C, Abercrombie H, Schaefer S, Benca R, Davidson R (2004) Functional but not structural subgenual prefrontal cortex abnormalities in melancholia. Mol Psychiatry 9:393–405.

Pourtois G, Dan ES, Grandjean D, Sander D, Vuilleumier P (2005) Enhanced extrastriate visual response to bandpass spatial frequency filtered fearful faces: time course and topographic evoked-potentials mapping. Hum Brain Mapp 26:65–79.

Previc F (1988) The neurophysiological significance of the N1 and P1 components of the visual evoked-potential. Clin Vis Sci 3:195–202.

Rhodes LJ, Ruiz A, Ríos M, Nguyen T, Miskovic V (2018) Differential aversive learning enhances orientation discrimination. Cogn Emot 32:885–891.

Rudvin I, Valberg A, Kilavik BE (2000) Visual evoked potentials and magnocellular and parvocellular segregation. Vis Neurosci 17:579–590.

Sacco T, Sacchetti B (2010) Role of secondary sensory cortices in emotional memory storage and retrieval in rats. Science 329:649–656.

Samogin J, Liu Q, Marino M, Wenderoth N, Mantini D (2019) Shared and connection-specific intrinsic interactions in the default mode network. Neuroimage 200:474–481.

Sasikumar D, Emeric E, Stuphorn V, Connor CE (2018) First-pass processing of value cues in the ventral visual pathway. Curr Biol 28:538–548.e3.

Schechter I, Butler PD, Zemon VM, Revheim N, Saperstein AM, Jalbrzikowski M, Pasternak R, Silipo G, Javitt DC (2005) Impairments in generation of early-stage transient visual evoked potentials to magno-and parvocellular-selective stimuli in schizophrenia. Clin Neurophysiol 116:2204–2215.

Sehlmeyer C, Schöning S, Zwitserlood P, Pfleiderer B, Kircher T, Arolt V, Konrad C (2009) Human fear conditioning and extinction in neuroimaging: a systematic review. PLoS One 4:e5865.

Stanislaw H, Todorov N (1999) Calculation of signal detection theory measures. Behav Res Methods Instrum Comput 31:137–149.
Steinberg C, Dobel C, Schupp HT, Kissler J, Elling L, Pantev C, Junghöfer M (2012) Rapid and highly resolving: affective evaluation of olfactorily conditioned faces. J Cogn Neurosci 24:17–27.
Stolarova M, Keil A, Moratti S (2006) Modulation of the C1 visual event-related component by conditioned stimuli: evidence for sensory plasticity in early affective perception. Cereb Cortex 16:876–887.
Thatcher R, North D, Biver C (2005) Evaluation and validity of a LORETA normative EEG database. Clin EEG Neurosci 36:116–122.
Thigpen NN, Bartsch F, Keil A (2017) The malleability of emotional perception: short-term plasticity in retinotopic neurons accompanies the formation of perceptual biases to threat. J Exp Psychol Gen 146:464–471.
Tobimatsu S, Tomoda H, Kato M (1995) Parvocellular and magnocellular contributions to visual evoked potentials in humans: stimulation with chromatic and achromatic gratings and apparent motion. J Neurol Sci 134:73–82.
Tolias AS, Keliris GA, Smirnakis SM, Logothetis NK (2005) Neurons in macaque area V4 acquire directional tuning after adaptation to motion stimuli. Nat Neurosci 8:591–593.
Tootell R, Hamilton SL, Switkes E (1988) Functional anatomy of macaque striate cortex. IV. Contrast and magno-parvo streams. J Neurosci 8:1594–1609.
Vitacco D, Brandeis D, Pascual-Marqui R, Martin E (2002) Correspondence of event-related potential tomography and functional magnetic resonance imaging during language processing. Hum Brain Mapp 17:4–12.
Weinberger NM (2004) Specific long-term memory traces in primary auditory cortex. Nat Rev Neurosci 5:279–290.
Weinberger NM (2007) Auditory associative memory and representational plasticity in the primary auditory cortex. Hear Res 229:54–68.
Weinberger NM (2011) The medial geniculate, not the amygdala, as the root of auditory fear conditioning. Hear Res 274:61–74.
Weinberger NM, Hopkins W, Diamond DM (1984) Physiological plasticity of single neurons in auditory cortex of the cat during acquisition of the pupillary conditioned response: I. Primary field (AI). Behav Neurosci 98:171–188.
Weinberger NM, Javid R, Lepan B (1993) Long-term retention of learning-induced receptive-field plasticity in the auditory cortex. Proc Natl Acad Sci U S A 90:2394–2398.
Whitton AE, Deccy S, Ironside ML, Kumar P, Beltzer M, Pizzagalli DA (2018) Electroencephalography source functional connectivity reveals abnormal high-frequency communication among large-scale functional networks in depression. Biol Psychiatry Cogn Neurosci Neuroimaging 3:50–58.
Wilcox RR (1987) New designs in analysis of variance. Annu Rev Psychol 38:29–60.
Wilson DA, Sullivan RM (2011) Cortical processing of odor objects. Neuron 72:506–519.
Worrell GA, Lagerlund TD, Sharbrough FW, Brinkmann BH, Busacker NE, Cicora KM, O'Brien TJ (2000) Localization of the epileptic focus by low-resolution electromagnetic tomography in patients with a lesion demonstrated by MRI. Brain Topogr 12:273–282.
Yang Y, Liu D-q, Huang W, Deng J, Sun Y, Zuo Y, Poo M-m (2016) Selective synaptic remodeling of amygdalocortical connections associated with fear memory. Nat Neurosci 19:1348–1355.
You Y, Li W (2016) Parallel processing of general and specific threat during early stages of perception. Soc Cogn Affect Neurosci 11:395–404.
Zinbarg RE, Mohlman J (1998) Individual differences in the acquisition of affectively valenced associations. J Pers Soc Psychol 74:1024–1040.
Zumsteg D, Friedman A, Wennberg RA, Wieser HG (2005) Source localization of mesial temporal interictal epileptiform discharges: correlation with intracranial foramen ovale electrode recordings. Clin Neurophysiol 116:2810–2818.